ELSEVIER

Biophysical Chemistry 124 (2006) 222–228

Biophysical Chemistry

http://www.elsevier.com/locate/biophyschem

Ab initio molecular dynamics study of the hydration of the formohydroxamate anion

Kevin Leung

Sandia National Laboratories, MS 1415, Albuquerque, NM 87185, United States

Received 18 January 2006; received in revised form 29 March 2006; accepted 1 April 2006
Available online 19 April 2006

Abstract

We apply ab initio molecular dynamics (AIMD) to study the hydration structures and electronic properties of the formohydroxamate anion in liquid water. We consider the *cis*- nitrogen-deprotonated, *cis*- oxygen-deprotonated, and *trans*- oxygen-deprotonated formohydroxamate tautomers. They form an average of 6.3, 6.9, and 6.0 hydrogen bonds with water molecules, respectively. The predicted pair correlation functions and time dependence of the hydration numbers suggest that water is highly structured around the nominally negatively charged oxime oxygen in O-deprotonated tautomers but significantly less so around the nitrogen atom in the N-deprotonated species. Wannier function analysis suggests that, in the O-deprotonated anions, the negative charge is concentrated on the oxime oxygen, while in the N-deprotonated case, it is partially delocalized between the nitrogen and the adjoining oxime oxygen atom.

Keywords: Ab initio molecular dynamics; Hydroxamic acids; Hydroxamate anion; Ion hydration

1. Introduction

Hydroxamic acids are weak acids that act as enzyme inhibitors and biomedical ligands [1] and are used as chelating agents for many metal ions in geochemical [2] and other environments [3]. Their chemistry is pertinent to macromolecules called siderophores secreted by bacteria to extract iron from minerals for metabolic purposes [4]. These applications are related to their strong affinity for certain metal ions. To provide a detailed understanding of the hydroxamic acid–metal binding in water, the hydration structures and electronic properties of the deprotonated forms of these acids are of significant interest.

Simple hydroxamic acids such as the formo-, aceto-, and benzo-species contain two acid protons, bonded to the oxime oxygen and the nitrogen sites. The preferred deprotonation site for acid molecules in liquid water is still in dispute. Experiments applying different spectroscopic methods, chemical substituents, solvents, and in some cases, N- and O-alkylation (thus preventing deprotonation at those sites), have reached differing conclusions or have suggested that both tautomers may be present [5–10]. On the theoretical side, Hartree Fock (HF), Møller–Plesset second-order (MP2), and semi-empirical quantum methods have shown that in the gas phase, formohydroxamic acid and acetohydroxamic acid preferentially deprotonate at the N-site [9–11]. In other words, they are "N-acids" (See Fig. 1c). This trend holds when a dielectric continuum model [10] or a semi-empirical quantum chemistry description using a gas phase cluster with four explicit water molecules [11] is used to mimic an aqueous environment solvating the hydroxamate anion, although both treatments predict that water stabilizes the O-deprotonated *cis*-tautomer more than the N-deprotonated one. Density Functional Theory (DFT) with the B3LYP exchange correlation functional [12,13] yields a similar relative stability for isolated hydroxamate anions in the gas phase [14]. On the other hand, a recent work combining infrared spectroscopy and DFT calculations conclude that acetohydroxamic acid deprotonates at the oxime O-site in water (i.e., an "O-acid") [15]. There, the B3LYP model includes three explicit water molecules and predicts that O-deprotonation is more favorable by 22.7 kcal/mol. Note that metal-chelation usually involves the O-deprotonated anions [2,3].

E-mail address: kleung@sandia.gov.

0301-4622/$ - see front matter © 2006 Elsevier B.V. All rights reserved.
doi:10.1016/j.bpc.2006.04.001

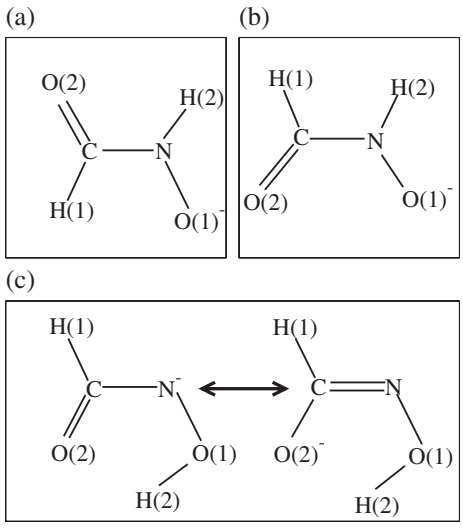

Fig. 1. (a and b) *trans*- and *cis*-formohydroxamic acid deprotonated at the oxime oxygen site; (c) *cis*- N-deprotonated formohydroxamate anion (two resonance structures shown). O(1) and O(2) are the oxime and carbonyl oxygens, respectively, while H(2) is the acid proton.

The present work applies ab initio molecular dynamics (AIMD) to study the hydration structures of three formohydroxamate anion tautomers (Fig. 1). Due to π-bond conjugation, these formohydroxamate conformers are fairly rigidly planar molecules, yielding substantial barriers towards rotation about the C–N bond. As a result, the *cis*- and *trans*-O-deprotonated species remain distinct and do not interconvert over the time scale of O(10) ps AIMD trajectories. Conversion between the O-deprotonated and N-deprotonated tautomers via water-mediated proton transfer does not occur on this time scale either. Thus, this study does not directly make predictions about the most favorable deprotonation site. However, by elucidating the number of hydrogen bonds formed between water and the anions, it can shed qualitative insight into how, and how favorably, water interacts with the hydroxamate tautomers. The predicted hydration number can pave the way for future quantum chemistry modeling of hydroxamate anions in cluster models using a full complement of first hydration shell water molecules [16], thus potentially lessening the dependence of the predicted anion stability on the number of explicit water molecules used [11,15]. The present work is also a prerequisite to the explicit computation of the potentials of mean force and free energy changes associated with isomerization between the N-deprotonation the O-deprotonation species via AIMD umbrella sampling [17,18], because the structures studied in this work are the end-points of the pertinent free energy curves.

In addition to understanding the acid–base properties of hydroxamic acids, the anion hydration structures are of inherent theoretical interest. The N-deprotonated tautomer, which has been shown to be stable in water, or at least stable enough to coexist with the O-acid anion form [6–10], has an unusual motif. It has several electronegative atoms in close proximity. It has been suggested that the nominal negative charge on nitrogen can be stabilized by the π-bond conjugation and resonance structure contributions (Fig. 1c). Resonance structures are also readily invoked for the O-deprotonated species [15]. To our knowledge, there has been no force field-based study that models hydroxamate anions in water. The present study yields insight not just into the hydration structure, enabling future force field modeling, but also considers the electron structure of the hydroxamate functional groups in liquid water. It may be pertinent to other aspects of hydroxamic acid–water interactions, such as water-mediated proton transfer [19].

This work is organized as follows. Section 2 applies AIMD to predict the hydration structures of three formohydroxamate anion tautomers/conformers. Section 3 briefly describes an analysis of the electronic structures of these anions in water using maximally localized Wannier functions [20]. Section 4 concludes this work with further discussions.

2. Methods

We conduct ab initio molecular dynamics using the Car–Parrinello Molecular Dynamics (CPMD) package [21]. We apply the Becke–Lee–Yang–Parr (BLYP) exchange correlation functional [13,22] and norm-conserving pseudopotentials. The simulation cells are cubic, of fixed lateral dimensions 12.4170 Å. They contain one formohydroxamate anion and 63 water molecules. Γ-point Brillouin zone sampling is used throughout. The wavefunction energy cutoff is set at 70 Ry, the frictitious electron mass used within the CPMD dynamics is 400 a.u., and the time step is 4 a.u. (0.0968 fs). The ions are thermostated at 300 K. The proton mass is used for all hydrogen atoms. It has been shown that these CPMD settings yield pair correlation functions for liquid water which agree with "Born–Oppenheimer" dynamics, i.e., AIMD simulations where the ground-state electronic wavefunctions are computed explicitly at each time step [23].

Each simulation is initiated by placing a hydroxamate anion tautomer in a box of 64 SPC/E water molecules [24] pre-equilibrated to 1.00 g/cm^3 water density. The one water molecule that overlaps with the anion is removed. This starting configuration is equilibrated at constant volume and an elevated temperature of 350 K using a 2-ps QM/MM trajectory, treating the anion with DFT while water remains as the SPC/E model. This QM/MM capability is implemented within the VASP code [25] and has been described and applied previously [26]. The final QM/MM configuration is then used as the initial geometry for a fully DFT-based AIMD simulation, where both water molecules and the anion are treated using the BLYP functional [13,22] and the CPMD code. After discarding the first 2–7 ps to allow the number of water molecules in the hydration shells of hydroxamate atoms to stabilize, statistics are collected over the next 10 ps.

Maximally localized Wannier orbital analyses are performed using the CPMD code [21]. We have also performed a few Gaussian [27] calculations on isolated hydroxamate anions with the 6–311+G(p,d) basis and the BLYP exchange correlation functional.

3. Ab initio molecular dynamics results

3.1. Hydration structures

The three formohydroxamate anion tautomers considered in this work are depicted in Fig. 1. It has been shown that Fig. 1c is the lowest energy structure in the gas phase, followed by Fig. 1a and b, in that order [10,11,14]. Since the liquid phase AIMD simulations apply the BLYP functional, and not B3LYP used in previous gas phase calculations [14], we have performed Gaussian [27] calculations at the BLYP/6–311+G(p,d) level of theory to confirm that BLYP is consistent with the B3LYP predictions of the gas phase relative stability. The optimal, zero-temperature BLYP energies for isolated *trans*- N-deprotonated, *trans*- O-deprotonated, and *cis*- O-deprotonated anions are 0.0, 7.5, and 10.0 kcal/mol, respectively, very similar to Remko's B3LYP/6-311+G(p,d) results [14], which we have also reproduced (0.0, 8.2, and 11.4 kcal/mol).

The pair correlation functions between water molecules and several atoms in *trans*- O-deprotonated formohydroxamate anion are depicted in Fig. 2. The oxime and carbonyl oxygens, O(1)and O(2), respectively, exhibit sharply peaked hydration structures, and the mean hydrogen bond lengths are 1.65 and 1.70 Å. The hydration numbers are N_w=3.1 and 2.1, respectively. N_w is computed by averaging the number of water protons within a 2.5-Å radius of each anion oxygen atom. The O(1)- and O(2)-water $g(r)$ (Fig. 2a and b) are qualitatively similar to those reported for formate anion oxygen atoms [26]. Quantitatively, compared to the two equivalent formate oxygens, each of which exhibits N_w=2.6 [26], we observe that the total numbers of hydrogen bonds formed by the two hydroxamate oxygens (5.1) and the carboxylate functional groups (5.2) are similar, but the negative charge of the anion is evidently more localized on O(1) in the present case, leading to

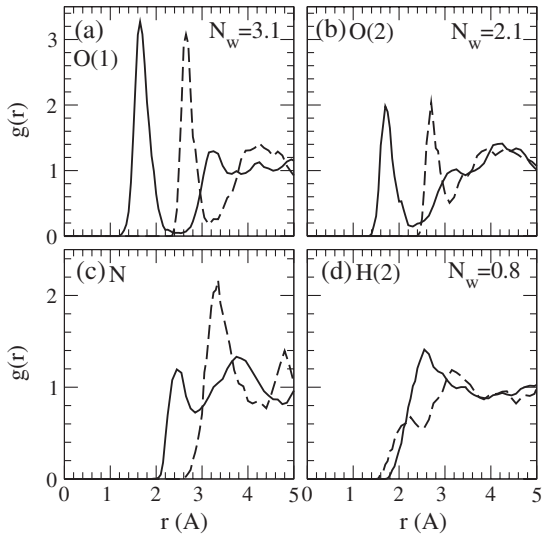

Fig. 2. Pair correlation functions g_{XH_w} (r) (solid line) and g_{XO_w} (r) (dashed) between *trans*-formohydroxamate anion atom 'X' and water H and O sites. (a) 'X'=oxime oxygen (O(1)); (b) carbonyl oxygen (O(2)); (c) nitrogen; (d) acid proton (H(2)).

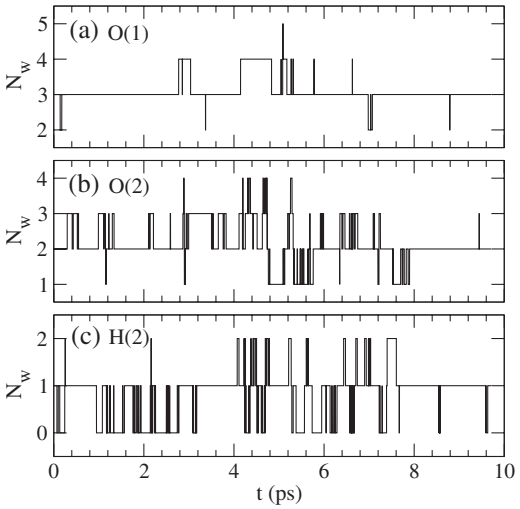

Fig. 3. Instantaneous number of hydrogen bonds N_w formed between water and *trans*- O-deprotonated formohydroxamate anion atoms. (a) Oxime oxygen (O(1)); (b) carbonyl oxygen (O(2)); (c) acid proton (H(2)).

sharp $g(r)$ peaks and a higher N_w for O(1) than for O(2). In fact, $g_{O(2)H_w}$ (r) (where H_w refers to water protons) and the associated N_w are qualitatively similar to those of carbonyl oxygens in neutral species like the uracil molecule [28]. The acid proton forms an average of 0.8 hydrogen bond with oxygen atoms on water molecules, using a simple criterion, namely, a 2.5 Å H–O_w cutoff distance.

Despite the non-zero $g_{NH_w}(r)$ for $r<2.5$ Å, the nitrogen atom is actually not hydrogen bonded to water. g_{NO_w} (r) and g_{NH_w} (r) do not peak at the typical distances of nitrogen–water hydrogen bonds (compare with Fig. 5, below). Instead, the first peak features in these $g(r)$ arise from the proximity of O(1) and its first hydration shell. If we count the total number of water molecules with protons within 2.5 Å of all three O(1), O(2), and N atoms, we obtain an average of 4.9. The same number emerges if only O(1) and O(2) are considered. This indicates that (a) N does not form direct hydrogen bonds; and (b) water molecules have a small but non-vanishing probability of simultaneously hydrogen bonding to O(1) and O(2). In the case of the *trans*- O-deprotonated hydroxamate anion, such simultaneous hydrogen bonding can only be achieved via a bridging geometry, where a water molecule sits atop the planar anion and its two protons interacts both with O(1) and O(2). The two oxygen atoms of the aqueous formate ion exhibits an even smaller tendency towards hydration sphere overlap, which is not discussed in Ref. [26].

Fig. 3 depicts the instantaneous hydration numbers exhibited by the *trans*- O-deprotonated formohydroxamate anion. The oxime oxygen is seen to have a relatively static hydration shell. Its N_w is predominately 3, with small temporal fluctuations, although there is actually one instance of a water molecule from the bulk liquid region displacing another originally in the first hydration shell within the 10 ps trajectory. The first hydration shells of the carbonyl oxygen and the acid proton are much more labile. Dividing these trajectories into 2 ps segments, we estimate standard deviations of ±0.1 in all reported N_w. The statistical uncertainties are likely underestimated because the

trajectory is not sufficiently long to perform a systematic blocking analysis.

We should point out that the BLYP exchange-correlation functional yields liquid structure for water at $T=300$ K and 1.0 g/cm^3 density when the zero point motion of the water protons are neglected [23,29–31]. However, our experience with $HCOO^-$ suggests that this overstructuring of bulk liquid water has only minor effects on the BLYP-predicted hydration number for monovalent ions. Thus, BLYP predicts significantly less liquid water structure at $T=350$ K and 1.0 g/cm^3 density than at ambient temperature, and the diffusion constant is also higher, in better agreement with experiments at $T=300$ K [31]. Despite this, $HCOO^-$ exhibits very similar average hydration numbers, respectively, 2.5 and 2.6 per formate oxygen, at $T=300$ K and $T=350$ K, although $g_{OH_w}(r)$ becomes less sharply peaked at the higher temperature [26]. This is apparently because water motion near the monovalent ion is still significant at $T=300$ K. Even at ambient temperature, we observe many transient fluctuations in the hydration numbers (Fig. 3). In addition, there are numerous instances of distinct water molecules entering and leaving the first hydration shells of various atoms. Thus, a total of 7, 9, and 10 distinct H_2O have entered the hydration shells of O(1), O(2), and H(2) within the 10-ps time-frame depicted in Fig. 3, respectively. Hence, N_w is apparently adequately sampled within an O(10) ps trajectory, despite the overstructuring of bulk liquid BLYP water at $T=300$ K. We note that water have far longer residence times in the hydration shells of divalent ions in general, and liquid water structure may play a stronger role in those cases.

In a similar vein, our experience with $HCOO^-$ [26] and other published results on the hydration of the dimethyl phosphate ion [32] suggest that the number of water molecules in the simulation cell at constant water density (thus, effectively increasing the anion "concentration") does not strongly affect the ion–water pair correlation functions or the total hydration number. In fact, even decreasing the water density by 7% changes the hydration number performate oxygen by only 0.1 units [33]. (The exchange correlation functional, on the other hand, appears to have stronger effects on N_w). Thus, we expect that N_w is an intrinsic property of ab initio molecular dynamics and is robust towards changing the simulation cell size.

Fig. 4 depicts some pair correlations of the *cis*- O-deprotonated formohydroxamate anion. Only the $g(r)$ substantially different from those of the *trans*-conformer are shown. O(1) exhibits $N_w=3.2$, and the $g(r)$ of this conformer (not shown)

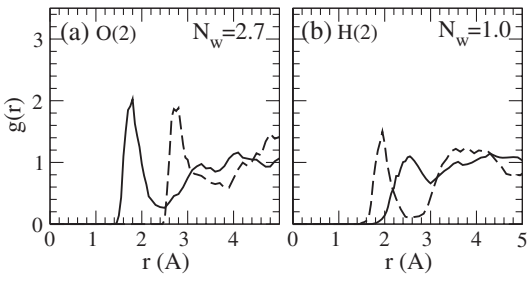

Fig. 4. $g(r)$ between *cis*-formohydroxamate anion atoms and water. (a) Carbonyl oxygen (O(2)); (b) acid proton (H2).

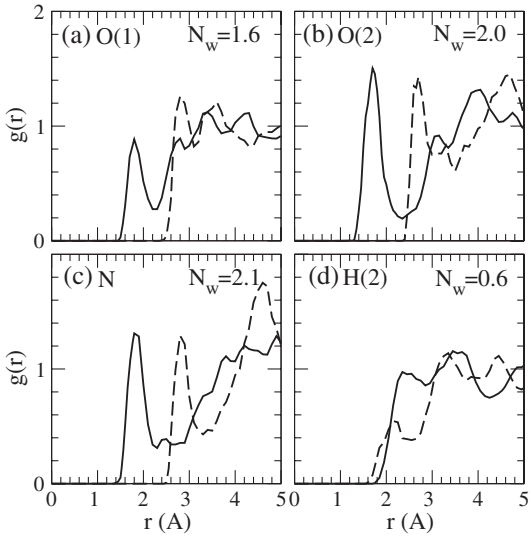

Fig. 5. Pair correlation functions $g_{XH_w}(r)$ (solid line) and $g_{XO_w}(r)$ (dashed) between N-deprotonated formohydroxamate anion atom 'X' and water H and O sites. (a) 'X'=oxime oxygen (O(1)); (b) carbonyl oxygen (O(2)); (c) nitrogen; (d) hydroxyl proton (H(2)).

are similar to those of the *trans*- form for this atom. The O(2) $g(r)$ (Fig. 4a) also appears qualitatively similar to those of the *trans*- form, but the N_w of this atom is increased to 2.7 due to contributions from the $2.0<r<2.5$ Å region. Despite this, the water molecules in the O(2) hydration shell remain labile, and the temporal fluctuations in N_w are similar to those in Fig. 3b. N_w for O(1) and O(2) add up to 5.9. There are an average of 5.6 water molecules in the hydration shells of O(1) and O(2), counting only once those instantaneously hydrogen bonded to both hydroxamate oxygens. Thus, there is an increase of 0.6 or 0.7 from the *trans*- case using either criterion. Qualitatively, the most significant difference between the *cis*- and *trans*- $g(r)$ is observed for H(2). The H(2)–O_w first peak is much more distinct in the *cis*- case, and the hydration number reaches $N_w=1.0$.

These differences are readily rationalized. In the *cis*-conformer, the two electronegative oxygens are aligned on one side of the anion while the electropositive acid proton is on the opposite side. This enhances the dipole moment of the anion and constructively reinforces the O(1)and O(2) interactions with protons on water molecules. From these structural considerations, we expect the *cis*-conformer to be more favorably hydrated in liquid water. This preference has been predicted using semi-empirical quantum chemistry calculations on a cluster model with one formohydroxamate anion and four explicit water molecules [11]. The same trend has been predicted for acetohydroxamate anions using the B3LYP functional and a cluster with three water molecules [15]. However, semi-empirical methods predict the opposite energy ordering for *cis*- and *trans*- O-deprotonated acetohydroxamate [11]. We conjecture that applying the full first hydration shell of water molecules predicted in this work to quantum chemistry cluster calculations may yield more consistent results.

Fig. 5 depicts the hydration structure of the *cis*- N-deprotonated tautomer. Here the oxime oxygen O(1) is

covalently bonded to an acid proton while nitrogen is not. The $g(r)$ between O(1) and water is much reduced from the O-deprotonated case, with N_w dropping to 1.6. N_w remains 2.1 for the carbonyl oxygen despite the fact that the first peaks in $g(r)$ are less sharply featured than in the O-deprotonated tautomers. The deprotonated nitrogen has $N_w = 2.0$. The nitrogen–water proton $g(r)$ peaks at 1.85 Å, a reasonable hydrogen bonding distance, in contrast to the amide nitrogen in the O-deprotonated tautomers (Fig. 2c). However, the nitrogen N_w is much smaller than that for O(1) in the O-deprotonated species. This suggests that water is not as strongly bound to the nominally negatively charged N as it is to O(1) in the O-deprotonated tautomer. This may be due to (a) a strong contribution from the resonance structure on the right-hand side of Fig. 1c, which reduces the net charge on N; (b) steric hindrance; and/or (c) delocalization of the negative charge to O(1). We consider these rationales briefly. (a) The O(2) of this tautomer exhibits N_w similar to those on the *trans*- O-deprotonated tautomer as well as carbonyl oxygens in neutral molecules [28], and its $g_{O(2)H_w}(r)$ is not strongly peaked. These observations suggest that the negative charge of the anion is not strongly localized on O(2), and that the resonance structure depicted on the right side of Fig. 1c does not contribute significantly in water. (b) The nitrogen atom is covalently bonded to both O(1) and a carbon, which should indeed sterically hinders hydrogen bonding between this atom and water. (c) As will be discussed in the next section, there is some degree of charge delocalization on to O(1).

The evolution of N_w on N and O(1) (Fig. 6 a and b) is consistent with the structural findings. Unlike the nominally negatively charged O(1) in O-deprotonated hydroxamate anions, there are numerous fast fluctuations in the nitrogen hydration number. Instantaneously, these individual atom-based N_w can add up to as much as 7 or as little as 2. Some of these are due to the exchange of first hydration shell water molecules between N and O(1). Because of their close proximity, a distance-based, $r < 2.5$ Å hydrogen bond criterion will yield a significant probability that a water molecule resides in the N and O(1) hydration shells simultaneously. Fig. 6c plots the total number of water molecules in the combined hydration shells of the two, after removing this double counting. This quantity exhibits much smaller (±1) fluctuations about its average value of 3.1. Even with the removal of double-counting, the temporal fluctuations are still much faster than those around the nominally negatively charged O(1) site in the *trans*- O-deprotonated anion (Fig. 3a). This corroborates the $g(r)$ evidence that water is not as strongly bound to the nitrogen atom in this anion as it is to O(1) in the O-deprotonated tautomers. Recalling that the N_w of N and O(1) add up to 3.6 compared to the no double counting average of 3.1 (Fig. 6c), we indeed find a significant overlap between the N and O(1) hydration shells.

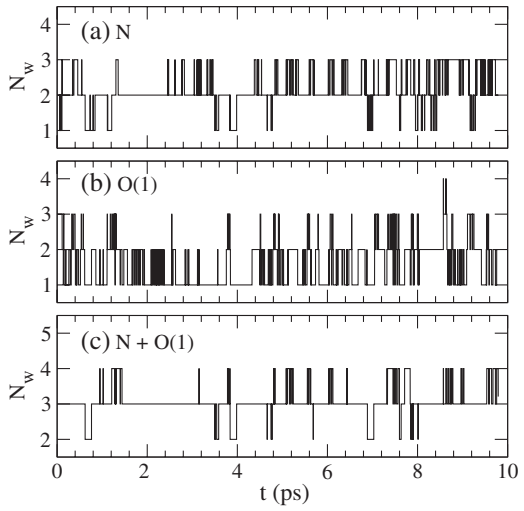

Fig. 6. (a and b) Instantaneous N_w for (a) nitrogen (N) and (b) oxime oxygen (O (1)) atoms, respectively, in *cis*- N-deprotonated formohydroxamate anion. (c) The total number of water molecules in the hydration shells of N and/or O(1), without double counting (see text).

To our knowledge, no X-ray or neutron scattering data are available to compare with the predicted hydration numbers. We note that counting the total number of hydrogen bonds (i.e., allowing double counting of water molecules) may be useful for interpreting future X-ray scattering data, which reflect the pairwise correlation between *individual* atoms of the anion and oxygen sites on water molecules. This criterion of hydration number is also a useful guideline for thermodynamic properties. For example, a water proton should prefer to be in the vicinity of two electronegative atoms rather than one. Similarly, a water molecule with both its protons hydrogen bonded to different negatively charged atoms on the same anion may be more strongly bound compared to H_2O forming just one hydrogen bond. With these two definitions, i.e., allowing/removing double counting of water molecules, the total hydration number on the nitrogen, oxygens, and acid protons add up to 6.3 and 5.8 for the N-deprotonated tautomer. The difference in total N_w between the *cis* N-deprotonated and the *cis* O-deprotonated tautomers is not large—only 0.6 and 0.8, respectively.

While the number of hydrogen bonds between a solute and water does not directly translate into a free energy prediction, the small difference in hydration numbers between the *cis*- O-deprotonation and the *cis*- N-deprotonated tautomers suggests that the 22.7 kcal/mol preference for the former species predicted in Ref. [15] is overestimated. Recall that the B3LYP functional predicts a 11.4 kcal/mol preference for the isolated *cis*- N-deprotonated tautomer over the *cis*- O-deprotonated form. So the results of Ref. [15], based on a cluster with one anion plus three water molecules, would imply that the O-deprotonated form interacts more favorably with water by 34.1 kcal/mol. The binding energy between a water molecule and an organic anion in the gas phase is of order ~20 kcal/mol. With more than one H_2O present in the first hydration shell, the average hydrogen bond energy per water molecule becomes even less. Thus, it would be difficult to reconcile a 34.1 kcal/mol hydration free energy difference between N-deprotonated and O-deprotonated hydromate anions, and the less than one hydrogen bond difference observed in the present AIMD trajectories. While we acknowledge that Ref. [15] focuses on the acetohydroxamate anion rather than formohydramate, the hydration structures of the two anions is not expected to be very different.

3.2. Wannier function analysis

In this section, we apply the maximally localized Wannier orbital [20] technique to examine the charge distributions on the *trans*- O-deprotonated and *cis*- N-deprotonated formohydroxamate anions. There are 24 valence electrons in formohydroxamate anion, filling 12 valence orbitals. These are decomposed into Wannie orbitals in one representative snapshot along each of the AIMD trajectory for the two species. Fig. 7 depicts these tautomers from two perspectives (in-plane and sideways), with each of the 12 orbitals plotted only once. Water molecules are removed for clarity. This figure shows that, in both cases, the C–N bond has pronounced π- or double-bond character, indicating some degree of resonance behavior (e.g., the right hand side of Fig. 1c). However, the carbon–carbonyl oxygen (O(2)) bond also retains a pronounced double bond character in both cases. In the O-deprotonated form, we find no tendency of double bond formation or π-bonding between the nominally negatively charged O(1) and N. The most significant difference between the electronic structures of the two tautomers is that the N–O σ-bonding orbital electron density is more equitably shaded between O(1) and N in the O-deprotonated case, whereas it is more localized on the oxime oxygen in the N-deprotonated case. In particular, the centers of charge of Wannier orbitals can be uniquely elated to the polarization and dipole moment of a system. The center of charge of the N–O σ-bonding orbital lies along the N–O(1) axis. In the snapshot of the O-deprotonated tautomer, it is almost equidistant between N and O(1) and is located 0.74 and 0.71 Å away from these atoms, respectively. In the N-deprotonated case, these distances are 0.90 and 0.66 Å, confirming the visual evidence in Fig. 7 that the electron cloud is significantly shifted on to O(1). (The N–O bond length in this snapshot is also significantly longer (1.55 Å) than the O-deprotonated case (1.44 Å) due to differences in the covalent bonding). This suggests that the negative charge on the N-deprotonated anion is delocalized over the nitrogen and O(1) atoms to some extent.

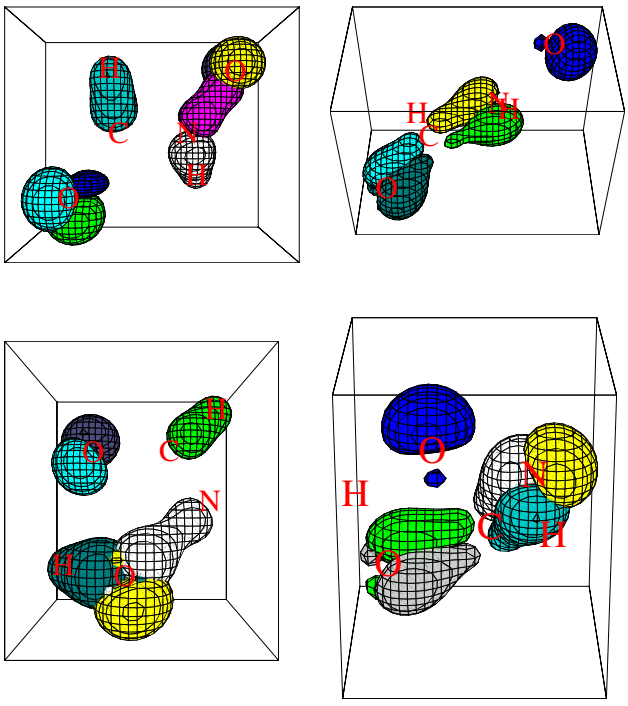

Fig. 7. Snapshots of maximally localized Wannier orbitals. Upper panels: two views of *trans*- O-deprotonated formohydroxamate anion; lower panels: *cis*- N-deprotonated formohydroxamate. Each set refers to the same snapshot along the AIMD trajectory, but from different (flat vs. sideways) perspectives. The regions occupied by each of the 12 Wannier orbitals are depicted in a different color in each panel, and each orbital is shown only once for each structure. The N–O(1), C–H(1), and N–H(2) (or O–H(2)) σ-bonds are depicted in the left panels, while the C–O(2) and C–N double bonds are shown in the right panels. H_2O molecules are removed for clarity.

These inferences are drawn by examining representative snapshots. Nevertheless, the apparent charge sharing between N and O(1) in the N-deprotonated species is consistent with our analysis based on examining $g(r)$ (Figs. 2 and 5) and the temporal fluctuations of the hydration numbers (Figs. 3 and 6) of the different tautomers.

4. Conclusions

In conclusion, we have applied ab initio molecular dynamics to study three formohydroxamate anion tautomers known to be among the most stable in the gas phase. The O-deprotonated species in general exhibit more sharply featured $g(r)$ for the oxime oxygen atoms. The *cis*-conformer exhibits larger hydration numbers than the *trans*-conformer, consistent with the fact that its two aligned oxygen atoms yield a large dipole moment and favor a stronger interaction with water molecules. The combined hydration numbers N_w for O(1), O(2), and H(2) for *trans*- and *cis*- O-deprotonated formohydroxamate anion are 6.0 and 6.9, respectively. For the *cis*- N-deprotonated formohydroxamate tautomer, N_w for O(1), O(2), N and H(2) add up to 6.3. The N and O(2) atoms are in close proximity and exhibit enhanced probability of sharing and exchanging water molecules in their hydration shells. The fluctuations in hydration numbers for these atoms are much faster than those for the nominally negatively charged O(1) in the O-deprotonated anions. The electron densities of the tautomers in water are analysed using a maximally localized Wannier orbital decomposition. Significant double bond character is found for the carbon–carbonyl oxygen and carbon–nitrogen bonds in both O-deprotonated and N-deprotonated tautomers. The N–O(1) σ-bond electron density is shifted towards the oxygen atom in the N-deprotonated case and suggests partial delocalization of the negative charge to O(1). Our predicted hydration numbers may lead to future, more accurate quantum chemistry calculations which apply the AIMD-predicted full complement of first hydration shell water molecules to cluster models.

Acknowledgement

We thank Ann Mattsson and Dubravko Sabo for their kind assistance. This work was supported by the Department of

Energy under Contract DE-AC04-94AL85000. Sandia is a multiprogram laboratory operated by Sandia Corporation, a Lockheed Martin Company, for the U.S. Department of Energy.

References

[1] C.J. Marmion, D. Griffth, K.B. Nolan, Eur. J. Inorg. Chem. (2004) 3003.
[2] B.A. Holmén, M.I. Tejedor-Tejedor, W.H. Casey, Langmuir 13 (1997) 2197.
[3] L. Morroni, F. Secco, M. Venturini, B. Garcia, J.M. Leal, Inorg. Chem. 43 (2004) 3005 (and references therein).
[4] T. Palanche, S. Blanc, C. Hennard, M.A. Abdallah, A.M. Albrecht-Gary, Inorg. Chem. 43 (2004) 1137.
[5] H.L. Yale, Chem. Rev. 33 (1943) 209.
[6] R.E. Plapinger, J. Org. Chem. 24 (1959) 802.
[7] J. Gerstein, W.P. Jencks, J. Am. Chem. Soc. 86 (1964) 4655.
[8] L. Bauer, O. Exner, Angew. Chem., Int. Ed. Engl. 13 (1974) 376.
[9] A. Bagno, C. Comuzzi, G. Scorrano, J. Am. Chem. Soc. 116 (1994) 916.
[10] M.L. Senent, A. Niño, C.M. Caro, S. Ibeas, B. Garcia, J.M. Leal, F. Secco, M. Venturini, J. Org. Chem. 68 (2003) 6535.
[11] O.N. Ventura, J.B. Rama, L. Turi, J.J. Dannenberg, J. Am. Chem. Soc. 115 (1993) 5754.
[12] A.D. Becke, J. Chem. Phys. 98 (1993) 5648.
[13] C.T. Lee, W.T. Yang, R.G. Parr, Phys. Rev., B 37 (1988) 785.
[14] M. Remko, J. Phys. Chem., A 106 (2002) 5005.
[15] D.C. Edwards, S.B. Nielsen, A.A. Jarzecki, T.G. Spiro, S.C.B. Myneni, Geochim. Cosmochim. 69 (2005) 3237.
[16] L.R. Pratt, S.B. Rempe, in: L.R. Pratt, G. Hummer (Eds.), Simulation and Theory of Electro-Static Interations in Solution, ALP, New York, 1999, pp. 172–201.
[17] K. Leung, S.B. Rempe, J. Chem. Phys. 122 (2005) 184506.
[18] J.E. Davis, N.L. Doltsinis, A.J. Kirby, C.D. Roussev, M. Sprik, J. Am. Chem. Soc. 124 (2002) 6594.
[19] S.J. Yen, C.Y. Lin, J.J. Ho, J. Phys. Chem., A 104 (2000) 11771.
[20] N. Marzari, D. Vanderbilt, Phys. Rev., B 56 (1997) 12847;
P.L. Silvestrelli, Phys. Rev., B 59 (1999) 9703.
[21] CPMD Version 3.4, J. Hütter, P. Ballone, M. Bernasconi, P. Focher, E. Fois, S. Goedecker, D. Marx, M. Parrinello, M. Tuckerman, MPI für Festkörperforschung and IBM Research Laboratory (1990–1998), Copyright IBM 1990, 1997, Copyright MPI 1997.
[22] A.D. Becke, Phys. Rev., A 38 (1988) 3098.
[23] I.F.W. Kuo, C.J. Mundy, M.J. McGrath, J.I. Siepmann, J. Vande Vondele, M. Sprik, J. Hutter, B. Chen, M.L. Klein, M. Mohamed, M. Krack, M. Parrinello, J. Phys. Chem., B 108 (2004) 12990.
[24] H.J.C. Berendsen, J.R. Gridera, T.P. Straatsma, J. Phys. Chem. 91 (1987) 6269.
[25] G. Kresse, J. Furthmüller, Phys. Rev., B 54 (1996) 11169;
G. Kresse, J. Furthmüller, Comput. Mater. Sci. 6 (1996) 15.
[26] K. Leung, S.B. Rempe, J. Am. Chem. Soc. 126 (2004) 344.
[27] M.J. Frisch, et al., Gaussian 98 (Revision A.2), Gaussian Inc., Pittsburgh, PA, 1998.
[28] M.P. Gaigeot, M. Sprik, J. Phys. Chem., B 108 (2004) 7458.
[29] D. Asthagiri, L.R. Pratt, J.D. Kress, Phys. Rev., E 68 (2003) 415051.
[30] J.C. Grossman, E. Schwegler, E.W. Draeger, F. Gygi, G. Galli, J. Chem. Phys. 120 (2004) 300.
[31] J. VandeVondele, F. Mohamed, M. Krack, J. Hutter, M. Sprik, M. Parrinello, J. Chem. Phys. 122 (2005) 014515.
[32] I.F. Kuo, D.J. Tobias, J. Phys. Chem., B 105 (2001) 5827.
[33] K. Leung, S.B. Rempe, Phys. Chem. Chem. Phys 8 (2006) 2153–2162.